



## **Effect of Activated Carbon on Re-Conversion Reaction of Cu/LiCl/C Electrode with LiPF<sub>6</sub>/Methyl Difluoroacetate Electrolyte**

**Katsuo Hashizaki<sup>1,2\*</sup>, Shinsaku Dobashi<sup>2,3</sup>, Shigeto Okada<sup>1</sup>, Toshiro Hirai<sup>2</sup>,  
Jun-ichi Yamaki<sup>2</sup> and Zempachi Ogumi<sup>2</sup>**

<sup>1</sup>*Institute for Materials Chemistry and Engineering, Kyushu University, 6-1 Kasuga-Koen,  
Kasuga, Fukuoka 816-8580, Japan.*

<sup>2</sup>*Office of Society-Academia Collaboration for Innovation, Kyoto University, Uji-shi,  
Kyoto 611-0011, Japan.*

<sup>3</sup>*Research and Innovation Center, Mitsubishi Heavy Industries, Ltd., Nagasaki-shi,  
Nagasaki 851-0392, Japan.*

### **Authors' contributions**

*This work was carried out in collaboration between all authors. Author KH designed the study, performed the statistical analysis, wrote the protocol and wrote the first draft of the manuscript. Authors SD, SO, TH, JIY and ZO managed the analyses of the study. All authors read and approved the final manuscript.*

### **Article Information**

DOI: 10.9734/CJAST/2019/46501

#### Editor(s):

(1) Dr. Santiago Silvestre, Associate Professor, Telecommunications Engineering, Universitat Politècnica de Catalunya, Spain.

#### Reviewers:

(1) Christos N. Panagopoulos, National Technical University of Athens, Greece.

(2) J. Guillermo Soriano-Moro, Universidad Autónoma de Puebla, México.

Complete Peer review History: <http://www.sdiarticle3.com/review-history/46501>

**Original Research Article**

**Received 19 October 2018**

**Accepted 09 January 2019**

**Published 19 January 2019**

### **ABSTRACT**

Transition-metal chlorides are known to suffer from dissolution in organic solvents. However, our previous investigation revealed that in the Li/CuCl<sub>2</sub> battery, the dissolution of CuCl<sub>2</sub> cathode materials could be suppressed by using LiPF<sub>6</sub>/methyl difluoroacetate (MFA; CHF<sub>2</sub>COOCH<sub>3</sub>) electrolyte. And, the Cu/LiCl electrode could both charge and discharge in LiPF<sub>6</sub>/methyl difluoroacetate (MFA) electrolyte as the re-conversion reaction cathode of Li/CuCl<sub>2</sub> battery. However, the capacity is only half the theoretical value of 399 mAh g<sup>-1</sup>. This is because cuprous is hardly oxidized to cupric during charging due to copper disproportionation reaction.

\*Corresponding author: E-mail: 3ES16003G@s.kyushu-u.ac.jp, k-hashizaki@iae.or.jp;

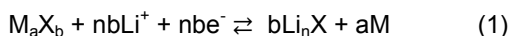
In this study, activated carbon was added to the Cu/LiCl electrode in order to promote the production of CuCl<sub>2</sub>, and to improve the capacity. The physical properties of the activated carbon were found to have significant effects: activated carbon with a large specific surface area and micropore volume enabled CuCl<sub>2</sub> deposition, and improved the capacity of the Cu/LiCl/C electrode to approximately 300 mAh g<sup>-1</sup>.

*Keywords: Lithium ion battery; Li/CuCl<sub>2</sub> battery; MFA; activated carbon, conversion; re-conversion.*

## 1. INTRODUCTION

Lithium-ion batteries (LIBs) are being widely used in electronic applications (e.g., portable devices), electrical vehicles (EVs), electric energy storage system (EES or ESS), and electrical power control system of photovoltaic and/or wind-turbine power generation. Both existing and new applications demand ever higher performance in LIBs, in terms of energy density, power, volume, safety, price, and environmental impact [1-3]. Currently, the electrical energy density of conventional LIBs is approaching the theoretical limit, which is imposed by the intercalation/de-intercalation mechanism of Li<sup>+</sup> ions in the host material. In order to achieve 2–5 times the current energy density needed for future applications, LIBs based on new concepts are required.

Many studies have been conducted on improving the cathode, anode, and electrolyte materials in LIBs [4-10]. The main limiting factors for the capacity are the phase stability of these materials, and the number of lithium ions exchanged. One new research focus is cathode materials based on conversion reactions. In conventional electrode materials, the Li<sup>+</sup> intercalation/de-intercalation processes do not change the material's crystal structure. In contrast, the conversion-type materials undergo complete structural and chemical changes during charge and discharge. Such a process involves a much larger number of electrons, which enable them to achieve extremely high capacities. Specifically, the conversion reaction related to an irreversible structural change can be expressed by the following equation [7].



where M is a transition metal (Cu, Fe, Co, Ni, Bi, etc.), X is an anion (O, F, S, N, P, etc.), and b is the formal oxidation state of X (n = 1–3). Redox reactions (1) between the cathode material M<sub>a</sub>X<sub>b</sub> and Li<sup>+</sup> ions involve the full reduction of the transition metals to their metallic states in the cathode, thereby delivering remarkably higher

capacity than intercalation-based LIBs. The Li/CuCl<sub>2</sub> battery is attractive in terms of its high voltage (3.07 V vs. Li<sup>+</sup>/Li) and high theoretical capacity (399 mAh g<sup>-1</sup>) due to the two-electron redox reactions of CuCl<sub>2</sub> + 2Li<sup>+</sup> + 2e<sup>-</sup> ⇌ Cu + 2LiCl. Li/CuCl<sub>2</sub> batteries also exhibit lower overvoltage at discharge and charge, compared to other conversion-based LIBs. However, transition-metal chlorides have received little attention for conversion-based LIBs, due to their propensity for dissolution in non-aqueous electrolytes [11,12]. Nevertheless, our recent studies revealed that the electrolyte LiPF<sub>6</sub>/methyl difluoroacetate (MFA) is effective for suppressing the self-discharge in Li/CuCl<sub>2</sub> batteries [13].

Meanwhile, many studies have been conducted on the electrochemical properties of batteries using Li/transition-metal fluorides [14-25], sulfides [26-40], and oxides [41-54]. Most of the published results are concerned with discharge starting from the M<sub>a</sub>X<sub>b</sub> electrode, while very few focus on charge starting from the M/Li<sub>n</sub>X electrode [55,56]. If the charge-starting re-conversion-based LIBs could be realized by using the M/Li<sub>n</sub>X electrode, there would be the new possibilities of Li storage and the adoption of graphite as the anode. During the re-conversion reaction, the Li<sup>+</sup> ions are supplied by Li<sub>n</sub>X in the cathode. Therefore, the Li metal anodes can be substituted by graphite anodes, leading to greatly enhanced battery safety. Since the conventional intercalation-type LIB already uses graphite anodes, merely changing the cathode to the M/Li<sub>n</sub>X electrode can create the conversion reaction-based cell with much higher energy density. In the Li/CuCl<sub>2</sub> batteries, this would mean charge starting from the Cu/LiCl or Cu/LiCl/C electrodes as re-conversion reaction cathodes, instead of discharge starting from the CuCl<sub>2</sub>/C electrode.

In a previous paper, charge and discharge on the Cu/LiCl electrode were found to be possible in LiPF<sub>6</sub>/MFA electrolyte even without additional carbon in the electrode. Nevertheless, the resulting low capacity (150 mAh g<sup>-1</sup>) requires improved CuCl<sub>2</sub> formation. In industrial corrosion

control, activated carbon is commonly used to remove adsorbed chlorine ions in aqueous solutions in order to protect copper metal. Therefore, we expect that in the Cu/LiCl electrode, the chlorine ion concentration (activity) in the reaction field for CuCl<sub>2</sub> formation can be similarly controlled by adding carbon-based adsorbents. In this work, we investigate the influence of different carbon additives on the charge-starting Cu/LiCl/C re-conversion reaction cathodes for LIBs. We also examine the effect of LiPF<sub>6</sub>/MFA on the formation/deposition of CuCl<sub>2</sub>, and on improving Cu utilization efficiency and charge/discharge capacities. The mechanisms of the re-conversion reaction in Cu/LiCl/C electrode with LiPF<sub>6</sub>/MFA are proposed as follows: micropores in the added carbon control the ion concentrations in the electrochemical reaction field, especially that of the chlorine ion, thereby promoting the formation of CuCl<sub>2</sub>.

## 2. EXPERIMENTAL DETAILS

Cu/LiCl and Cu/LiCl/C electrodes and LiPF<sub>6</sub>/MFA electrolyte were prepared under dry conditions (O<sub>2</sub> concentration: < 1 ppm; dew point: < -80 °C) inside an Ar-filled glove box (Miwa Mfg. Co. Ltd.). The Cu/LiCl/C cathodes were prepared by mixing Cu powder (Kojundo Chemical Laboratory Co. Ltd, CUE08PB), anhydrous LiCl (Sigma-Aldrich Co. LLC, 429457-25G), a carbon material (glassy carbon (ALS Co., Ltd, S-12), activated carbon A (UES Co., Ltd, UCG-CPT) or B (Asahi Organic Chemicals Industry Co., Ltd, AC-0230)), and polytetrafluoroethylene (PTFE; Du Pont-Mitsui Fluorochemicals Co. Ltd., 6J).

The weight ratio was Cu:LiCl:C:PTFE = 32:48:15:5. The content of the CuCl<sub>2</sub>/acetylene black (AB) electrode was CuCl<sub>2</sub>:AB:PTFE=70:25:5, which corresponds to Cu:LiCl:C:PTFE=28:42:25:5 in the Cu/LiCl/C electrode. However, the AB particles have very different size from that of activated carbon. Considering that charge and discharge are possible in the carbonless Cu/LiCl electrode, we decided to use a lower ratio of carbon (15 wt%) in order to isolate the effect of Cl<sup>-</sup> adsorption on charge-discharge performance. Additionally, the actual performance was poor with 25 wt% activated carbon.

The Cu/LiCl cathode electrode was prepared by mixing Cu powder, anhydrous LiCl, and PTFE in a weight ratio of Cu:LiCl:PTFE = 40:50:10.

Prior to mixing, LiCl was ground in a mortar to crush the particles to ~10 micron in size. Each carbon material was dried at 200°C under vacuum condition for 24 h. The cathode materials were mixed in a mortar and rolled into a 150 μm-thick sheet. Discs (φ = 5 mm) were punched out of the sheet, and pressed onto a Pt mesh (Sanwakinzoku Co., 100 mesh) at 10 MPa to prepare the Cu/LiCl and Cu/LiCl/C electrodes. Pure lithium foil (thickness: 200 μm, Honjo Metal Co. Ltd.) was used as the counter electrode. MFA (Tokyo Chemical Industry Co. Ltd.) was used as the electrolyte solvent. Its water content was ≤ 50 ppm and the purity was > 99%. The Li salt, LiPF<sub>6</sub>, was dissolved in MFA at 2.2 mol L<sup>-1</sup>, as a previous study showed that this concentration produced the lowest self-discharge [13].

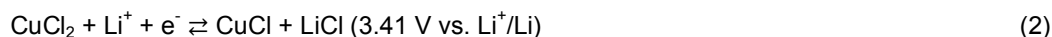
A three-electrode electrochemical cell (EC Frontier Co. Ltd.) was used for the charge/discharge measurements. The cell was assembled in Ar-filled glove box, with the cathode, counter electrode, and Li metal wire (φ = 1 mm, Honjo Metal Co. Ltd.) as the reference electrode. The charge and discharge measurements of the cell were performed sequentially in the glove box at room temperature with a potenti/galvanostat (Bio-Logic Science Instruments SAS, VSP-300, SP-200). The highest charge and lowest discharge voltages were 4.0 and 2.5 V, respectively, and the charge/discharge current rate was kept constant at 0.01 C.

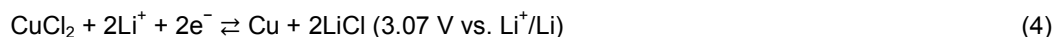
The microstructure of the Cu/LiCl/C electrode was characterized by X-ray diffraction (XRD; Bruker Co. D8 ADVANCE). The specific surface area and pore volume of each carbon material were measured by a high-precision gas/vapor adsorption measurement instrument (MicrotracBEL Corp. Belsorp-max), using Brunauer–Emmett–Teller (BET), t-plot, and Barrett–Joyner–Halenda (BJH) methods.

## 3. RESULTS AND DISCUSSION

### 3.1 Electrochemical Reactions of Li/CuCl<sub>2</sub> Batteries

The fundamental electrochemical reactions of Li/CuCl<sub>2</sub> batteries consist of the following single-electron redox reaction equations (2) and (3), which together can be described by the two-electron reaction in (4)





The formation and deposition of  $\text{CuCl}_2$  in reaction (2) are difficult, and the plateau at 3.4 V during discharge was scarcely seen in our previous study [13,57]. This would be caused by the disproportionation reactions with coexisting  $\text{Cu}^{2+}$ ,  $\text{Cu}^+$ , and  $\text{Cu}^0$ . Consequently,  $\text{CuCl}_2$  did not form or deposit on the electrode in the first discharge-charge process, according to X-ray absorption fine structure (XAFS) analysis. Only  $\text{CuCl}$  and  $\text{Cu}$  were detected when the cathode electrode was fully charged [57]. In this study, we investigate the possibility of using carbon additives in the cathode material to control the ion concentration in the electrochemical reaction fields.

The adsorptive property of activated carbon could suppress the dissolution of active materials in the  $\text{LiCl}/\text{C}$  electrode. The electrochemical reactions in the pores of activated carbon could also promote the formation and deposition of  $\text{CuCl}_2$ , and improve the  $\text{Cu}$  utilization efficiency. Consequently, the charge and discharge capacities could be increased.

### 3.2 Properties of Carbon Additives

The properties of the two activated carbon materials are shown in Table 1, with those of glassy carbon and acetylene black as references. Both activated carbon A and B have very high specific surface area and total pore volume (measured by BET method). The results of t-plot method indicate that the micropores were well-developed. The specific surface areas measured with BJH-method were used to assess the mesoporosity of the materials, which was quite high for A and B according to Table 1. In both activated carbons, the micropores were more developed than the mesopores, and the total specific surface area was mostly within the material (i.e., in pores) rather than on the surface. The micropores are expected to provide adequate sites for electrochemical reaction, and to suppress the dissolution of active cathode materials.

The properties of acetylene black (DENKA BLACK) are also listed in Table 1. However, its primary particles are very different in size. Therefore, it was excluded from electrochemical experiments in this study. The specific surface area of acetylene black is confirmed to depend

on the particle size, and the larger particle size requires a higher content to create a sufficiently large specific surface area. However, the nonporous AB particles contained little internal or external pores according to its adsorption isotherms; therefore it is not suitable as an additive in the  $\text{Cu}/\text{LiCl}$  electrodes.

### 3.3 Charge and Discharge Characteristics of $\text{Cu}/\text{LiCl}/\text{C}$ Composite

The charge and discharge profiles of the  $\text{Cu}/\text{LiCl}$  electrode ( $\text{Cu}:\text{LiCl}:\text{PTFE} = 40:50:10$ ) with 2.2 M  $\text{LiPF}_6/\text{MFA}$  is shown in Fig. 1 as a reference. This electrode was verified as a feasible re-conversion reaction cathode with  $\text{LiPF}_6/\text{MFA}$  for charge and discharge, without using carbon as conductive additive in the preceding paper. The ratio of  $\text{Cu}:\text{LiCl}$  was chosen to be stoichiometric for synthesizing  $\text{CuCl}_2$ , and the capacity was based on the total weight of  $\text{Cu}$  and  $2\text{LiCl}$  within the electrode. The as-prepared  $\text{Cu}/\text{LiCl}$  electrode had poor conductivity; therefore, the charged voltage was high and the charged capacity low during the first charge-discharge cycle. However, from the second cycle on, this electrode could be charged without the excess voltage shown in the initial cycle. The reason is that the fine copper particles precipitated on the electrode to form an electron transfer path, thereby acting as a conductive material in place of carbon.

However, the capacity of the  $\text{Cu}/\text{LiCl}$  electrode only reached half of its theoretical capacity ( $399 \text{ mAh g}^{-1}$ ). The obvious plateau at 2.7 V was attributed to the electrochemical reaction in equation (3), while the mild plateau at about 3.4 V was attributed to equation (2). The plural electrochemical reactions, such as  $\text{CuCl} \rightarrow \text{Cu}^{2+} + \text{Cl}^- + \text{e}^-$  (3.6 V vs.  $\text{Li}^+/\text{Li}$ ), and/or  $\text{Cu} \rightarrow \text{Cu}^+ + \text{e}^-$  (3.6 V vs.  $\text{Li}^+/\text{Li}$ ) would occur at the same time in the charge process. During discharge, an initial plateau at 3.4 V corresponding to reaction (2) was observed, but it was not extended. The plateau at 2.7 V was observed clearly. These behaviors are assumed to be due to the copper disproportionation reactions.

Fig. 2 shows the charge and discharge profiles of the  $\text{Cu}/\text{LiCl}/\text{C}$  electrodes with  $2.2 \text{ mol L}^{-1}$   $\text{LiPF}_6/\text{MFA}$ , where C = glassy carbon.

**Table 1. Physical properties of different carbon materials used in the Cu/LiCl/C electrode. Glassy carbon and acetylene black are listed as references**

|   | Acetylene black | Glassy carbon | Activated carbon A | Activated carbon B |
|---|-----------------|---------------|--------------------|--------------------|
| Specific surface area (BET, m <sup>2</sup> /g)          | 55              | 2             | 1780               | 2960               |
| Primary particle size (μm)                              | 0.043           | 5.0           | 6.5                | 2.2                |
| Total pore volume (BET, cm <sup>3</sup> /g)             | 0.18            | 0             | 0.86               | 1.9                |
| Average pore diameter (nm)                              | 13.2            | 11            | 1.9                | 2.5                |
| Total specific surface area (t-plot, m <sup>2</sup> /g) | 63              | 3             | 1700               | 3710               |
| •Outer  | —               | —             | 60                 | 72                 |
| •Inner  | —               | —             | 1640               | 3640               |
| Inner pore volume (t-plot, cm <sup>3</sup> /g)          | —               | 0             | 0.75               | 1.7                |
| Specific surface area (BJH, m <sup>2</sup> /g)          | 59              | 2.3           | 241                | 1460               |
| Total Pore volume (BJH, cm <sup>3</sup> /g)             | 0.3             | 0             | 0.24               | 1.0                |

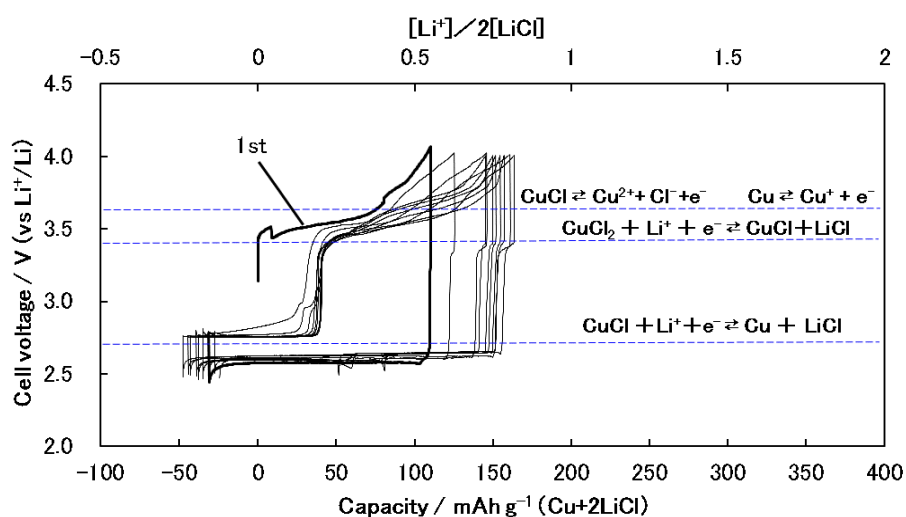


**Fig. 1. Charge and discharge profiles of the Cu/LiCl electrode in LiPF<sub>6</sub>/MFA electrolyte**

The overvoltage in the initial charge became lower with glassy carbon. After the second charge process, the clear plateau at 2.7 V was observed first. The mild sloping plateau near 3.4 V became more extended which would be attributed to the simultaneous electrochemical reactions, such as  $\text{CuCl} + \text{LiCl} \rightarrow \text{CuCl}_2 + \text{Li}^+ + \text{e}^-$  (3.4 V vs.  $\text{Li}^+/\text{Li}$ ),  $\text{CuCl} \rightarrow \text{Cu}^{2+} + \text{Cl}^- + \text{e}^-$  (3.6 V vs.  $\text{Li}^+/\text{Li}$ ), and/or  $\text{Cu} \rightarrow \text{Cu}^+ + \text{e}^-$  (3.6 V vs.  $\text{Li}^+/\text{Li}$ ). The extension of the sloping plateau at 3.4 V suggests that  $\text{CuCl}_2$  formation and deposition could occur on the Cu/LiCl/C electrode. Accordingly, a plateau at 3.4 V due to Cu reduction (2) was observed during discharge, and the total capacity also increased to nearly 250  $\text{mAh g}^{-1}$ .

As shown in Table 1, even though glassy carbon consisted of large particles with very few pores

and a smaller specific surface area, its presence effectively increased the charged capacity due to the enhanced formation and deposition of  $\text{CuCl}_2$  with equation (2). The increased  $\text{CuCl}_2$  deposition would also enhance the conductivity of the Cu/LiCl/C electrode, as explained earlier. The capacity of  $\sim 250 \text{ mAh g}^{-1}$  could be further improved by using carbon additives with more suitable properties.

Fig. 3 shows the charge and discharge profiles of the Cu/LiCl/C electrode with C = activated carbon A. The overvoltage in the initial charge process became lower than that in glassy carbon (Fig. 2), and the plateaus at 3.2 V and near 3.4 V appeared clearly in the initial charge process. The plateau at 3.2 V would be attributed to the electrochemical reaction of  $\text{Cu} + \text{Cl}^- \rightarrow \text{CuCl} + \text{e}^-$  (3.2 V vs.  $\text{Li}^+/\text{Li}$ ). This reaction seems to be

caused by LiCl, which is slightly soluble in the Cu/LiCl/C electrode. The second mild slope plateau near 3.4 V would be attributed to reaction (2), as discussed above. The plateau at about 3.6 V would be attributed to the plural electrochemical reactions  $\text{CuCl} \rightarrow \text{Cu}^{2+} + \text{Cl}^- + \text{e}^-$ , and/or  $\text{Cu} \rightarrow \text{Cu}^+ + \text{e}^-$ .

A comparison of Fig. 2 and Fig. 3 shows that the second mild slope plateau near 3.4 V appeared clearly in the charge process with glassy carbon and activated carbon A. In the discharge process, the plateau at 3.4 V attributed to the Cu reduction reaction (2) became more extended in

Fig. 3. The large specific surface area and pore volume (especially that from micropores) of activated carbon A are believed affect the ion concentration (especially that of  $\text{Cl}^-$ ) in an electrochemical reaction field, thereby promoting the formation and deposition of  $\text{CuCl}_2$  and suppressing the dissolution of active cathode materials. Following repeated charge and discharge, the plateau at 3.2 V gradually shifted to 3.4 V and disappeared, because the corresponding reaction was hindered by the accumulated deposits (e.g. LiF) at the opening of the micropores in the activated carbon.

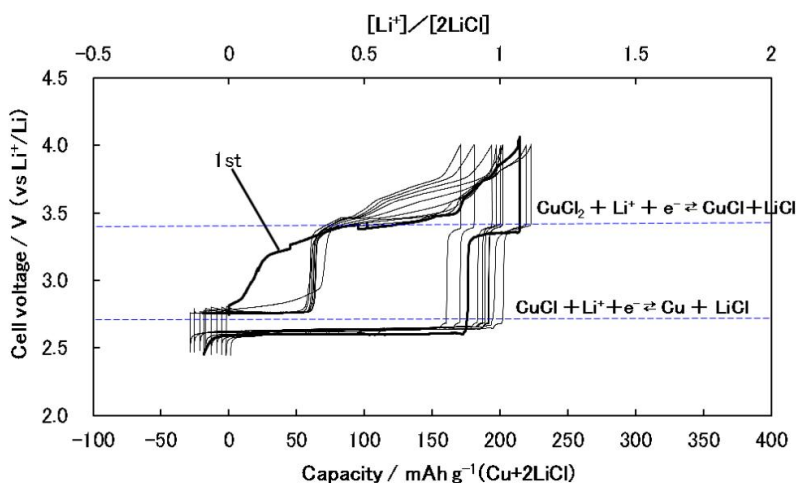


Fig. 2. Charge and discharge profiles of the Cu/LiCl/C electrode, with C = glassy carbon

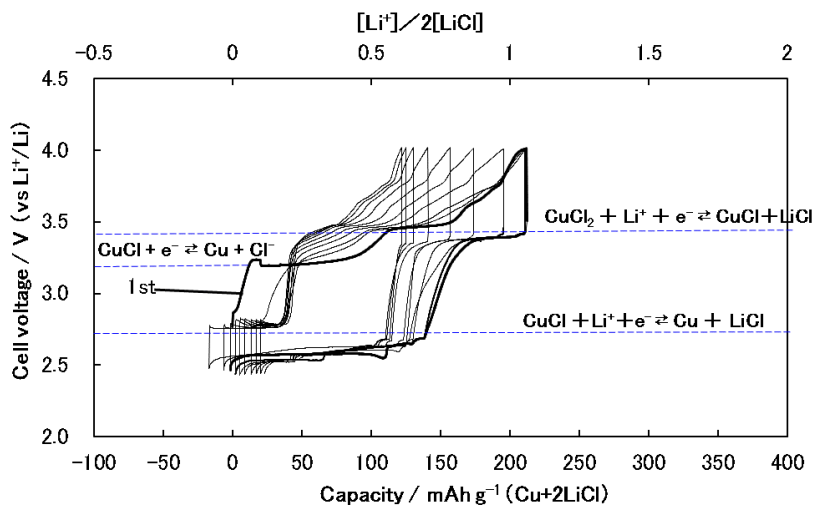


Fig. 3. Charge and discharge profiles of the Cu/LiCl/C electrode, with C = activated carbon A

Fig. 4 shows the charge and discharge profiles of the Cu/LiCl/C electrode using activated carbon B. Compared to activated carbon A (Fig. 3), the overvoltage in the initial charge was lowered, and the plateaus at 3.2 V and ~3.4 V appeared more clearly and extended further compared to activated carbon (Fig. 3). The charge capacity was increased to near 300 mAh g<sup>-1</sup>.

The main difference between Fig. 3 and Fig. 4 is the length of each plateau, with the longer plateau corresponding to higher capacity. Change of the plateau at 3.4 V especially contributes to the increased total capacity. According to these figures and Table 1, the larger the specific surface area and pore volume, the longer the plateaus at 3.2 and 3.4 V in the initial charge, and also the longer the plateau of 3.4 V due to Cu reduction reaction (2) in the discharge process.

Thus, we confirmed that the specific surface area and pore volume of the carbon additive greatly influence the electrochemical reactions in the charge and discharge processes of the Cu/LiCl/C electrode. This occurs through changing the ion concentration in electrochemical reaction fields, especially within the micropores. While the LiPF<sub>6</sub>/MFA electrolyte suppressed the dissolution of active materials, the activated carbon was confirmed to promote the formation and deposition of CuCl<sub>2</sub> and to further suppress the dissolution of active cathode materials. However, data in Fig. 4 show a gradual decline in these improvements, presumably due to the capture of

reactants in the micropores. It is important to address this problem in the future.

Next, we discuss the effect of the microstructure of carbon materials (namely the specific surface area and pore volume) on the formation and deposition of CuCl<sub>2</sub>. From Fig. 5, the initial discharge capacity corresponding to the Cu reduction reaction (2) (3.4 V) has good linear correlation with the specific surface area of the carbon material. Thus, activated carbon with large specific surface area strongly promotes the formation and deposition of CuCl<sub>2</sub>. A similar linear relationship is visible in Fig. 6, between the initial discharge capacity and the pore volume of the carbon material in each Cu/LiCl/C electrode. Hence, the pore volume of activated carbon also strongly influences the formation and deposition of CuCl<sub>2</sub>. A plausible explanation for the above correlations is as follows. The development of micropores increased the specific surface area of the carbon material. The ion concentration in the electrochemical reaction fields can be readily changed within the micropores, thereby enabling the formation of CuCl<sub>2</sub> that could not be achieved previously. Other carbon materials rich in micropores, such as carbon nanotubes, are expected to have similar effects.

To verify that CuCl<sub>2</sub> was actually formed and deposited in the Cu/LiCl/C electrode at the full charged condition, the XRD patterns of Cu/LiCl/C electrode after the initial charge are displayed in Fig. 7, together with the typical patterns of CuCl<sub>2</sub> and CuCl for reference.

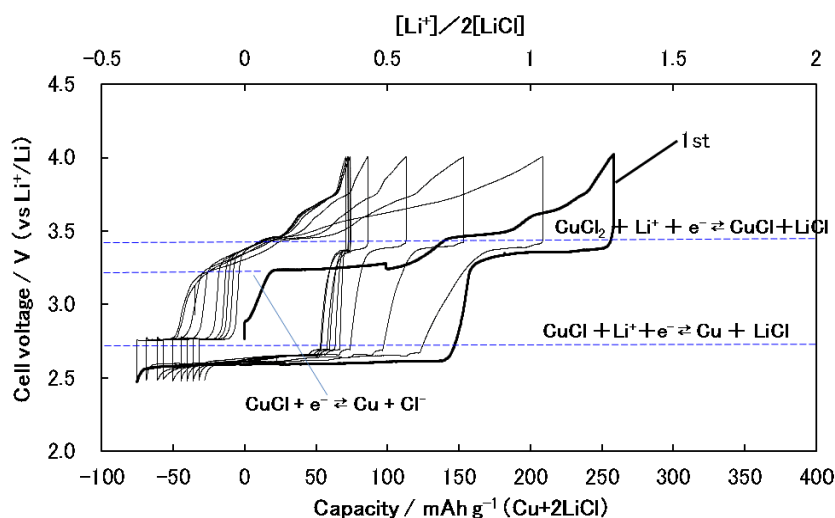


Fig. 4. Charge and discharge profiles of the Cu/LiCl/C electrode, with C = activated carbon B

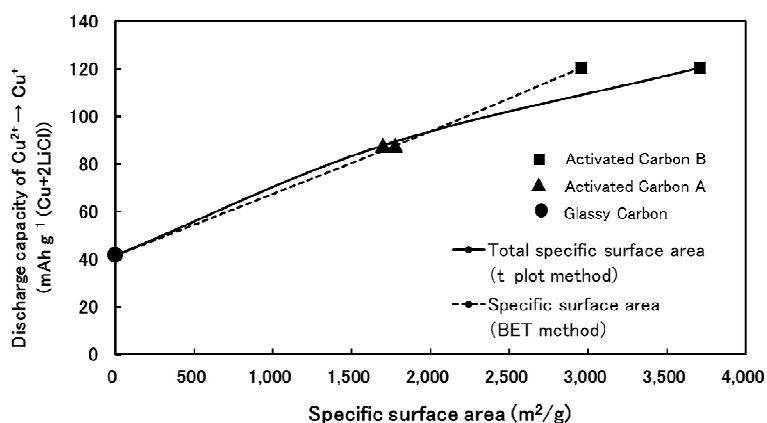


Fig. 5. Relationship between the initial discharge capacity corresponding to Cu reduction reaction (2), and the specific surface area of the carbon additive

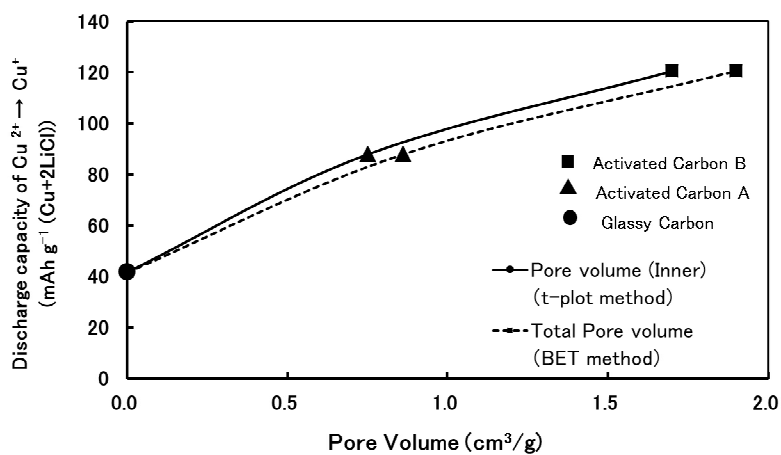


Fig. 6. Relation to initial discharge capacities that correspond to the Cu reduction, equation (2), and pore volumes of activated carbons in each Cu/LiCl/C electrode

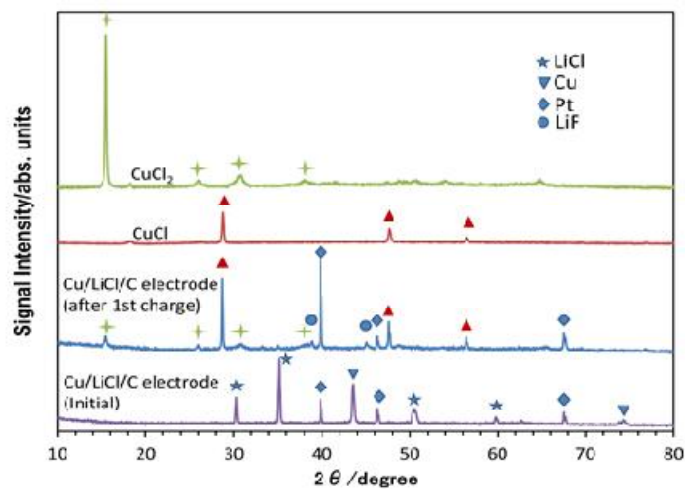


Fig. 7. XRD patterns of the Cu/LiCl/C electrode after the initial charge, CuCl<sub>2</sub>, and CuCl



Previous studies of the Cu/LiCl electrode under the fully charged condition only showed signals of CuCl and Cu, not CuCl<sub>2</sub> [57]. When activated carbon B was added, CuCl<sub>2</sub> signal was confirmed together with that of CuCl. Presumably, the reaction forming CuCl<sub>2</sub> would occur in pores, especially the micropores of activated carbon. The pores also helped to suppress the dissolution of active cathode materials, thereby facilitating CuCl<sub>2</sub> deposition on the Cu/LiCl/C electrode.

#### 4. CONCLUSION

This study used activated carbon in the Cu/LiCl electrode to enhance the CuCl<sub>2</sub> formation, and the following results were obtained.

- 1) Similar to the Cu/LiCl electrode, the Cu/LiCl/C electrode containing activated carbon can also charge-discharge as re-conversion reaction cathodes with LiPF<sub>6</sub>/MFA electrolyte. The charged capacity was improved from 200 to 300 mAh g<sup>-1</sup>.
- 2) The discharge plateau at 3.4 V (vs Li<sup>+</sup>/Li) corresponding to CuCl<sub>2</sub> + Li<sup>+</sup> + e<sup>-</sup> → CuCl + LiCl was observed. The specific surface area and pore volume (especially the micropore volume) of additive carbon are linearly correlated with the capacity in the initial discharge process.
- 3) XRD analysis confirmed that the Cu/LiCl/C electrode with activated carbon contained CuCl<sub>2</sub> after full charge, which is believed to be formed and deposited within the micropores.
- 4) Other porous carbon materials such as carbon nanotubes are expected to have similar functions as activated carbon.

#### COMPETING INTERESTS

Authors have declared that no competing interests exist.

#### REFERENCES

1. Dunn B, Kamath H, Tarascon JM. Electrical energy storage for the grid. A Battery of Choices. *Science*. 2011;334: 928-935.
2. Etacheri V, Marom R, Elazari R, Salitra G, Aurbach D. Challenges in the development of advanced Li-ion batteries. A review. *Energy Environ. Sci*. 2011; 4:3243-3262.
3. Tarascon JM, Armand M. Issues and challenges facing rechargeable lithium batteries. *Nature*. 2001;414:359-367.
4. Goriparti S, Miele E, De Angelis F, Di Fabrizio E, Zaccaria RP, Capiglia C. Review on recent progress of nanostructured anode materials for Li-ion batteries. *J. Power Sources*. 2014; 257:421-443.
5. Zhou YN, Xue MZ, Fu ZW. Nanostructured thin film electrodes for lithium storage and all-solid-state thin-film lithium batteries. *J. Power Sources*. 2013;234:310-332.
6. Scrosati B, Garche J. Lithium batteries: Status, prospects and future. *J. Power Sources*. 2010;195:2419-2430.
7. Cabana J, Monconduit L, Larcher D, Palacin MR. Beyond intercalation-based li-ion batteries: The state of the art and challenges of electrode materials reacting through conversion reactions. *Adv. Mater*. 2010;22:E170-E192.
8. Palacin MR. Recent advances in rechargeable battery materials: A chemist's perspective. *Chem. Soc. Rev*. 2009;38:2565-2575.
9. Malini R, Uma U, Sheela T, Ganesan M, Renganathan NG. Conversion reactions: A new pathway to realise energy in lithium-ion battery—review. *Ionics*. 2009; 15:301-307.
10. Bruce PG, Scrosati B, JM. Tarascon nanomaterials for rechargeable lithium batteries. *Angew. Chem. Int. Ed*. 2008; 47:2930-2946.
11. Liu JL, Cui WJ, Wang CX, Xia YY. Electrochemical reaction of lithium with CoCl<sub>2</sub> in nonaqueous electrolyte. *Electrochem. Commun*. 2011;13:269-271.
12. Li T, Chen ZX, Cao YL, Ai XP, Yang HX, Transition-metal chlorides as conversion cathode materials for li-ion batteries. *Electrochim. Acta*. 2012;68:202-205.
13. Dobashi S, Hashizaki K, Yakuma H, Hirai T, Yamaki J, Ogumi Z. Suppression of self-discharge by a LiPF<sub>6</sub>/Methyl difluoroacetate electrolyte in Li/CuCl<sub>2</sub> batteries. *J. Electrochem. Soc*. 2015; 162(14):A2747-A2752.
14. Arai H, Okada S, Sakurai Y, Yamaki J. Cathode performance and voltage estimation of metal trihalides. *J. Power Sources*. 1997;68:716-719.

15. Badway F, Pereira N, Cosandey F, Amatucci GG. Carbon-metal fluoride nanocomposites structure and electrochemistry of  $\text{FeF}_3\text{:C}$ . *J. Electrochem. Soc.* 2003;150(9):A1209-A1218.
16. Badway F, Cosandey F, Pereira N, Amatucci GG. Carbon metal fluoride nanocomposites high-capacity reversible metal fluoride conversion materials as rechargeable positive electrodes for li batteries. *J. Electrochem. Soc.* 2003; 150(10):A1318-A1327.
17. Li H, Balaya P, Maier J. Li-storage via heterogeneous reaction in selected binary metal fluorides and oxides. *J. Electrochem. Soc.* 2004;151(11):A1878-A1885.
18. Fu ZW, Li CL, Liu WY, Ma J, Wang Y, Qin QZ. Electrochemical reaction of lithium with cobalt fluoride thin film electrode. *J. Electrochem. Soc.* 2005;152(2):E50-E55.
19. Plitz I, Badway F, Al-Sharab J, DuPasquier A, Cosandey F, Amatucci GG. Structure and electrochemistry of carbon-metal fluoride nanocomposites fabricated by solid-state redox conversion reaction. *J. Electrochem. Soc.* 2005;152(2):A307-A315.
20. Makimura Y, Rougier A, Laffont L, Womes M, Jumas JC, Leriche JB, Tarascon JM. Electrochemical behaviour of low temperature grown iron fluoride thin films. *Electrochem. Commun.* 2006;8:1769-1774.
21. Badway F, Mansour AN, Pereira N, Al-Sharab JF, Cosandey F, Plitz I, Amatucci GG. Structure and electrochemistry of copper fluoride nanocomposites utilizing mixed conducting matrices. *Chem. Mater.* 2007;19:4129-4141.
22. Zhang H, Zhou YN, Sun Q, Fu ZW. Nanostructured nickel fluoride thin film as a new Li storage material. *Solid State Sci.* 2008;10:1166-1172.
23. Li T, Li L, Cao YL, Ai XP, Yang HX. Reversible three-electron redox behaviors of  $\text{FeF}_3$  nanocrystals as high-capacity cathode-active materials for Li-Ion batteries. *J. Phys. Chem. C.* 2010; 114:3190-3195.
24. Li C, Gu L, Tsukimoto S, van Aken PA, Maier J. Low-temperature ionic-liquid-based synthesis of nanostructured iron-based fluoride cathodes for lithium batteries. *Adv. Mater.* 2010; 22:3650- 3654.
25. Yamakawa N, Jiang M, Grey CP. Investigation of the conversion reaction mechanisms for binary copper (ii) compounds by solid-state NMR spectroscopy and X-ray diffraction. *Chem. Mater.* 2009;21:3162-3176.
26. Bonino F, Lazzari M, Rivolta B, Scrosati B. Electrochemical behavior of solid cathode materials in organic electrolyte lithium batteries: Copper Sulfides. *J. Electrochem. Soc.* 1984;131(7):1498-1502.
27. Chung JS, Sohn HJ. Electrochemical behaviors of  $\text{CuS}$  as a cathode material for lithium secondary batteries. *J. Power Sources.* 2002;108:226-231.
28. Han SC, Kim HS, Song MS, Kim JH, Ahn HJ, Lee JY. Nickel sulfide synthesized by ball milling as an attractive cathode material for rechargeable lithium batteries. *J. Alloys Compd.* 2003;351:273-278.
29. Hayashi A, Ohtomo T, Mizuno F, Tadanaga K, Tatsumisago M. Rechargeable lithium batteries, using sulfur-based cathode materials and  $\text{Li}_2\text{S-P}_2\text{S}_5$  glass-ceramic electrolytes. *Electrochim. Acta.* 2004;50:893-897.
30. Yan JM, Huang HZ, Zhang J, Liub ZJ, Yang Y. A study of novel anode material  $\text{CoS}_2$  for lithium ion battery. *J. Power Sources.* 2005;146:264-269.
31. Debart A, Dupont L, Patrice R, Tarascon JM. Reactivity of transition metal (Co, Ni, Cu) sulphides versus lithium: The intriguing case of the copper sulphide. *Solid State Sci.* 2006;8:640-651.
32. Zhu XJ, Wen Z, Gu ZH, Huang SH. Room-temperature mechanochemical synthesis of  $\text{Ni}_3\text{S}_2$  as cathode material for rechargeable lithium polymer batteries. *J. Electrochem. Soc.* 2006;153(3):A504-A507.
33. Wang Q, Gao R, Li JH. Porous, self-supported  $\text{Ni}_3\text{S}_2/\text{Ni}$  nanoarchitected electrode operating through efficient lithium-driven conversion reactions. *Appl. Phys. Lett.* 2007;90(14):143107.
34. Matsumura T, Nakano K, Kanno R, Hirano A, Imanishi N, Takeda Y. Nickel sulfides as a cathode for all-solid-state ceramic lithium batteries. *J. Power Sources.* 2007;174:632-636.
35. Wang Q, Li JH. Facilitated lithium storage in  $\text{MoS}_2$  overlayers supported on coaxial carbon nanotubes. *J. Phys. Chem. C.* 2007;111:1675-1682.
36. Wang JZ, Chou SL, Chew SY, Sun JZ, Forsyth M, MacFarlane DR, Liu HK. Nickel sulfide cathode in combination with an

- ionic liquid-based electrolyte for rechargeable lithium batteries. *Solid State Ionics*. 2008;179:2379-2382.
37. Gomez-Camer JL, Martin F, Morales J, Sanchez L. Precipitation of CoS vs ceramic synthesis for improved performance in lithium cells. *J. Electrochem. Soc.* 2008;155(3):A189-A195.
  38. Takeuchi T, Sakaebe H, Kageyama H, Sakai T, Tatsumi K. Preparation of NiS<sub>2</sub> using spark-plasma-sintering process and its electrochemical properties. *J. Electrochem. Soc.* 2008;155(9):A679-A687.
  39. Li H, Li WJ, Ma L, Chen WX, Wang JM. Electrochemical lithiation/ delithiation performances of 3D flowerlike MoS<sub>2</sub> powders prepared by ionic liquid assisted hydrothermal route. *J. Alloys Compd.* 2009;471:442-447.
  40. Apostolova RD, Shembel EM, Talyosef I, Grinblat J, Markovsky B, Aurbach D. Study of electrolytic cobalt sulfide Co<sub>9</sub>S<sub>8</sub> as an electrode material in lithium accumulator prototypes. *Russ. J. Electrochem.* 2009;45(3):311-339.
  41. Poizot P, Laruelle S, Grugeon S, Dupont L, Tarascon JM. Nano-sized transition-metal oxides as negative-electrode materials for lithium-ion batteries. *Nature*. 2000;407(28):496-499.
  42. Grugeon S, Laruelle S, Herrera-Urbina R, Dupont L, Poizot P, Tarascon JM. Particle size effects on the electrochemical performance of copper oxides toward lithium. *J. Electrochem. Soc.* 2001;148(4):A285-A292.
  43. Larchera D, Sudanta G, Lerichea JB, Chabreb Y, Tarascon JM. The electrochemical reduction of Co<sub>3</sub>O<sub>4</sub> in a lithium cell. *J. Electrochem. Soc.* 2002;149(3):A234-A241.
  44. Dolle M, Poizot P, Dupont L, Tarascon JM. Experimental evidence for electrolyte involvement in the reversible reactivity of CoO toward compounds at low potential. *electrochem. Solid-State Lett.* 2002;5(1):A18-A21.
  45. Laruelle S, Grugeon S, Poizot P, Dolle M, Dupont L, Tarascon JM. On the origin of the extra electrochemical capacity displayed by MO/Li cells at low potential. *J. Electrochem. Soc.* 2002;149(5):A627-A634.
  46. Poizot P, Laruelle S, Grugeon S, Tarascon JM. Rationalization of the low-potential reactivity of 3d-metal-based inorganic compounds toward li. *J. Electrochem. Soc.* 2002;149(9):A1212-A1217.
  47. Yuan Z, Huang F, Feng C, Sun J, Zhou Y. Synthesis and electrochemical performance of nanosized Co<sub>3</sub>O<sub>4</sub>. *Mater. Chem. Phys.* 2003;79(1):1-4.
  48. Balaya P, Li H, Kienle L, Maier J. Fully reversible homogeneous and heterogeneous li storage in RuO<sub>2</sub> with high capacity. *Adv. Funct. Mater.* 2003;13(8):621-625.
  49. Hu J, Li H, Huang X. Cr<sub>2</sub>O<sub>3</sub>-based anode materials for li-ion batteries. *Electrochem. And Solid-State Lett.* 2005;8(1):A66-A69.
  50. Li WY, Xu LN, Chen J. Co<sub>3</sub>O<sub>4</sub> nanomaterials in lithium-ion batteries and gas sensors. *Adv. Funct. Mater.* 2005;15:851-857.
  51. Jiao F, Bao J, Bruce PG. Factors influencing the rate of Fe<sub>2</sub>O<sub>3</sub> conversion reaction. *Electrochem. and Solid-State Lett.* 2007;10(12):A264-A266.
  52. Kim J, Chung MK, Ka BH, Ku JH, Park S, Ryu J, Oh SM. The role of metallic fe and carbon matrix in Fe<sub>2</sub>O<sub>3</sub>/Fe/Carbon nanocomposite for lithium-ion batteries. *J. Electrochem. Soc.* 2010;157(4):A412-A417.
  53. Wadewitz D, Gruner W, Herklotz M, Klose M, Giebeler L, Voß A, Thomas J, Gemming T, Eckert J, Ehrenberg H. Investigation of copper-cobalt-oxides as model systems for composite interactions in conversion-type electrodes for lithium-ion batteries. *J. Electrochem. Soc.* 2013;160(8):A1333-A1339.
  54. Adam R, Wadewitz D, Gruner W, Klemm V, Ehrenberg H, Rafaja D. Phase and microstructure development in the conversion type electrodes for li-ion batteries based on the Cu-Fe-O system. *J. Electrochem. Soc.* 2013;160(9):A1594-A1603.
  55. Zhou Y, Liu W, Xue M, Yu L, Wu C, Wu X, Fu Z. LiF/Co nanocomposite as a new li storage material. *Electrochem. and Solid-State Lett.* 2006;9(3):A147-A150.
  56. Prakash R, Wall C, Mishra AK, Kubel C, Ghafari M, Hahn H, Fichtner M. Modified synthesis of [Fe/LiF/C] nanocomposite, and its application as conversion cathode material in lithium batteries. *J. Power Sources*. 2011;196:5936-5944.
  57. Dobashi S, Nakanishi K, Tanida H, Hashizaki K, Uchimoto Y, Hirai T, Yamaki

J, Ogumi Z. Communication—XAFS analysis of discharge/charge reactions on the Li/CuCl<sub>2</sub> battery cathode with

LiPF<sub>6</sub>/Methyl difluoroacetate electrolyte. J. Electrochem. Soc. 2016;163(5):A727-A729.

© 2019 Hashizaki et al.; This is an Open Access article distributed under the terms of the Creative Commons Attribution License (<http://creativecommons.org/licenses/by/4.0>), which permits unrestricted use, distribution, and reproduction in any medium, provided the original work is properly cited.

*Peer-review history:*

*The peer review history for this paper can be accessed here:  
<http://www.sdiarticle3.com/review-history/46501>*